Improved Decentralized Method for Control of Building Structures under Seismic Excitation

Tian-Wei Ma[1]; Jeremy Johansen[2]; Ning-Shou Xu[3]; and Henry T. Y. Yang, M.ASCE[4]

Abstract: A decentralized control method with improved robustness and design flexibility is proposed for reducing vibrations of seismically excited building structures. In a previous study, a control scheme was developed for multistory building models using nonlinear, decentralized control theory. This control method has now been improved in this study in that less information about material properties and geometrical parameters of the building is needed and the selection of control design parameters is more flexible. The nonlinear behavior of the proposed control system is studied and its stability property is proven mathematically. To evaluate the effectiveness and robustness of the proposed method, three illustrative structural models, i.e., an eight-story elastic shear beam model, a two-story nonlinear elastic shear beam model, and a 20-story elastic benchmark model are studied. The 1940 El Centro and the 1995 Kobe earthquakes are used in these examples. The performance of the current control design, as applied to these examples, has shown to be more effective in reducing structural responses and improving robustness.

DOI: 10.1061/(ASCE)EM.1943-7889.0000104

CE Database subject headings: Feedback control; Vibration; Buildings, Multistory; Earthquake resistant structures; Nonlinear systems; Seismic effects; Structural control.

Author keywords: Feedback control; Vibration; Multistory buildings; Earthquake resistant.

Introduction

Since the concept of using control methods to reduce structural vibrations due to external excitations was proposed in the 1960s (Yao 1972; Yang 1975), a vast amount of research efforts in structural control have been devoted to the development of a variety of control algorithms based on different control design criteria. Some examples include: classical optimal control (Martin and Soong 1976), pole assignment (Rohman and Leipholz 1978), covariance control (Lu and Skelton 1998), multiobjective control (Johnson et al. 1998; Whorton et al. 1998; Brown et al. 1999), sliding mode control (Adhikari et al. 1998; Wu et al. 1998), robust control (D'Amato and Rotea 1998; Balas 1998; Young and Bienkiewicz 1998), and predictive control (Xu and Yang 1999; Mei et al. 2001). Research effort has also been devoted to the implementation of these control schemes using various control devices such as active (Reinhorn et al. 1992) and semiactive devices (Dyke et al. 1998). Recently, attempts to employ decentralized control methods in buildings have explored alternative methods (Lynch and Law 2002; Nishitani et al. 2003; Xu et al. 2003).

In this study, a modified decentralized control technique based on the theory of sliding mode control is presented for applications to seismically excited civil infrastructures, such as multistory buildings. Unlike the previously developed method (Ma et al. 2008), prior, detailed knowledge about the structural parameters, such as material properties and geometric parameters, is no longer required in order that greater model uncertainty can be accommodated. The applicability of the proposed approach to structural control is demonstrated and its stability property analytically studied. Design guidelines are drawn from a qualitative analysis of the nonlinear behavior of the system. Finally, the effectiveness of the method in reducing vibrations and its robustness to factors such as variation of structural parameters and nonlinearities are studied using numerical examples.

Problem Formulation

The equations of motion of an $\mathbf{n}$-story building structure subjected to external excitations and control forces can be written as

$$\mathbf{M}\ddot{\mathbf{x}} + \mathbf{C}\dot{\mathbf{x}} + \mathbf{K}(\mathbf{x})\mathbf{x} = \mathbf{B_0} \cdot \mathbf{u} + \mathbf{G} \cdot \ddot{x}_g(t) \tag{1}$$

where $\mathbf{M}$, $\mathbf{C}$, and $\mathbf{K}(\mathbf{x})$=mass, damping, and stiffness matrices, respectively. Symbol $\mathbf{x}$ represents the $\mathbf{n}\times\mathbf{1}$ vector of structural displacement relative to the ground. Symbol $\mathbf{B}_0$ denotes an $\mathbf{n}\times\mathbf{r}$ matrix of control force position ($\mathbf{r}\leqslant\mathbf{n}$). Symbol $\mathbf{u}$ is the $\mathbf{r}\times\mathbf{1}$ vector of control force. Symbol $\mathbf{G}$ denotes the excitation location matrix defined by $\mathbf{G}=-\mathbf{M}\cdot\mathbf{1}$, where $\mathbf{1}$ is a $\mathbf{n}\times\mathbf{1}$ vector with all elements being unity. Symbol $\ddot{x}_g$ represents the time history of the ground acceleration components of an earthquake.

In this study, it is assumed that actuators are placed between floors so that they apply a pair of forces to the connecting floors

[1]Assistant Professor, Dept. of Civil and Environmental Engineering, Univ. of Hawaii at Manoa, Honolulu, HI 96822 (corresponding author). E-mail: tianwei@hawaii.edu

[2]Research Assistant, Dept. of Mechanical and Environmental Engineering, Univ. of California, Santa Barbara, CA 93106.

[3]Visiting Professor, Dept. of Civil and Environmental Engineering, Univ. of Hawaii at Manoa, Honolulu, HI 96822.

[4]Professor, Dept. of Mechanical and Environmental Engineering, Univ. of California, Santa Barbara, CA 93106.

Note. This manuscript was submitted on September 4, 2009; approved on October 14, 2009; published online on April 15, 2010. Discussion period open until October 1, 2010; separate discussions must be submitted for individual papers. This paper is part of the ***Journal of Engineering Mechanics***, Vol. 136, No. 5, May 1, 2010. ©ASCE, ISSN 0733-9399/2010/5-662–673/$25.00.

with the same magnitude but opposite direction. The actuator forces $\mathbf{f}$ that are exerted between floors, give a net force $\mathbf{u}$ on the floors, where

$$\mathbf{u} = \begin{bmatrix} \chi_1^{-1} & & & \\ -\chi_2^{-1} & \chi_2^{-1} & & \\ & -\chi_3^{-1} & \chi_3^{-1} & \\ & & \ddots & \ddots \end{bmatrix} \mathbf{f} = \Delta \cdot \mathbf{f} \tag{2}$$

in which χ_i^{-1} are related to the geometry of how the actuators are oriented between the floors. The inverse relationship is

$$\mathbf{f} = \begin{bmatrix} \chi_1^{-1} & & & \\ -\chi_2^{-1} & \chi_2^{-1} & & \\ & -\chi_3^{-1} & \chi_3^{-1} & \\ & & \ddots & \ddots \end{bmatrix}^{-1} \mathbf{u} = \begin{bmatrix} \chi_1 & & & \\ \chi_1 & \chi_2 & & \\ \chi_1 & \chi_2 & \chi_3 & \\ \vdots & \vdots & & \ddots \end{bmatrix} \mathbf{u} \tag{3}$$

For use in a chevron brace, $\chi_i^{-1}=1$, thus

$$f_i = \sum_{j=1}^{i} u_j \tag{4}$$

Using the total control force vector $\mathbf{u}$ in the control design formulation, $B_0=I_{\mathbf{n}}$ is an identity matrix of $\mathbf{n}\times\mathbf{n}$. Note that in the case where not every floor is equipped with actuators, the actuator force should be used for controller design and $B_0 \neq I_{\mathbf{n}}$.

Derivation of the proposed decentralized control strategy is based on the decomposition of the system dynamics of Eq. (1). A civil structure, e.g., a multistory building, can be considered as an entity of a number of connected substructures. Mathematically, the global system behavior reflects the resultant dynamics of these substructures coupled through interconnections. If the local dynamics of a single substructure are concerned, the effects of interconnections can be represented as additional external loads applied to the substructure. Feedback controllers designed based on the individual substructures result in a decentralized control implementation for the global structure. As the interconnections are not included in the local dynamics of the substructures, they are unknowns to these controllers. Thus, effective decentralized controllers based on substructuring must have the capability of accommodating such "unknown" loads in order to produce a desired global system behavior.

Assume that the structure is decomposed into N subsystems with every set of $\mathbf{n}_i$ adjacent stories being one of the subsystems, i.e., $\Sigma_{i=1}^{N}\mathbf{n}_i=\mathbf{n}$, $\mathbf{x}=[\mathbf{x}_1^{\mathrm{T}},\mathbf{x}_2^{\mathrm{T}},\ldots,\mathbf{x}_N^{\mathrm{T}}]$ and for every subsystem, there are $\mathbf{r}_i$ floors subjected to control forces; obviously $\mathbf{r}_i \leqslant \mathbf{n}_i$, $\mathbf{u}=[\mathbf{u}_1^{\mathrm{T}},\mathbf{u}_2^{\mathrm{T}},\ldots,\mathbf{u}_N^{\mathrm{T}}]$, and $\mathbf{B}_0=\mathrm{blockdiag}[\mathbf{B}_{01},\mathbf{B}_{02},\ldots,\mathbf{B}_{0N}]$, where $\mathbf{u}_i$ is the vector of control force for the ith subsystem. In this study, $\mathbf{r}_i=\mathbf{n}_i$, thus $\mathbf{B}_{0i}=\mathbf{I}_{\mathbf{n}_i}$. Note that depending on the definition of the local states $\mathbf{x}_i$, there are generally two natural ways of substructuring: $\mathbf{x}_i$ defined as interstory drifts or displacements relative to the ground. Since these two types of local states are linear mappings of each other, the equations of motion of the system are mathematically the same irrespective of the definition of the local states. However, when local states are used to define the control objective, the resulted controllers may be different.

Defining the local states to be relative to ground, the equations of motion of the ith subsystem can be written as

$$\mathbf{M}_i\ddot{\mathbf{x}}_i(t) + \mathbf{C}_i\dot{\mathbf{x}}_i(t) + \mathbf{K}_i(\mathbf{x}_i)\mathbf{x}_i = \tau_i, \quad i=1,2,\ldots,N \tag{5}$$

where $\mathbf{M}_i$, $\mathbf{C}_i$, and $\mathbf{K}_i$=mass, damping, and stiffness matrices of the ith system, respectively. The generalized force vector $\tau_i(t)$ is defined as (Ma et al. 2008)

$$\tau_i(t) = \mathbf{u}_i - \mathbf{z}_i(\mathbf{x},\dot{\mathbf{x}}) - \mathbf{d}_i, \quad \mathbf{d}_i = -\mathbf{G}_i\ddot{x}_g(t) \tag{6}$$

where $\mathbf{G}_i=-\mathbf{M}_i\cdot\mathbf{1}_{\mathbf{n}_i}$ and $\mathbf{z}_i(\mathbf{x},\dot{\mathbf{x}})$=vector of interconnection strength. Obviously, $\mathbf{z}_i(\mathbf{x},\dot{\mathbf{x}})$ and thus $\tau_i(t)$ depend on the states of all subsystems including the local states $\mathbf{x}_i$ and $\dot{\mathbf{x}}_i$. The objective of decentralized control is to design the controllers based on individual subsystems [Eq. (5)] such that only local feedback is needed for every controller and yet the global system response is reduced.

Decentralized Control Design

Define a sliding mode variable for every subsystem as

$$\bar{\mathbf{s}}_i \triangleq \dot{\mathbf{x}}_i + \Lambda_i\mathbf{x}_i = \dot{\mathbf{x}}_i - \dot{\mathbf{x}}_i^{\mathbf{r}}, \quad \dot{\mathbf{x}}_i^{\mathbf{r}} \triangleq -\Lambda_i\mathbf{x}_i \tag{7}$$

In this study, local controllers of the following form are proposed.

$$\mathbf{u}_i = -\mathbf{L}_i\bar{\mathbf{s}}_i + \mathbf{w}_i(\bar{\mathbf{s}}_i) \tag{8}$$

where $\mathbf{L}_i$=positive-definite linear local feedback gain of the ith subsystem to ensure the desired local dynamics of the subsystems and $\mathbf{w}_i(\bar{\mathbf{s}}_i)$=used to compensate for effects of uncertainties such as disturbances and interconnections so that the desired global behavior is achieved. Substituting Eq. (8) into Eq. (5) and considering definition (7) gives the closed-loop system equations of the ith subsystem as

$$\mathbf{M}_i\dot{\bar{\mathbf{s}}}_i + [\mathbf{C}_i+\mathbf{L}_i]\bar{\mathbf{s}}_i = -\mathbf{Y}_i\theta_i - \mathbf{z}_i(\mathbf{x},\dot{\mathbf{x}}) - \mathbf{d}_i + \mathbf{w}_i \tag{9}$$

where $\mathbf{Y}_i\theta_i=\mathbf{M}_i\ddot{\mathbf{x}}_i^{\mathbf{r}}+\mathbf{C}_i\dot{\mathbf{x}}_i^{\mathbf{r}}+\mathbf{K}_i(\mathbf{x}_i)\mathbf{x}_i$.

In this study, the local controllers are design such that the following positive-definite Lyapunov function is bounded, i.e., the resultant feedback system is globally stable

$$V(t) = \sum_{i=1}^{N} V_i(t) \triangleq \frac{1}{2}\sum_{i=1}^{N} \bar{\mathbf{s}}_i^T\mathbf{M}_i\bar{\mathbf{s}}_i \tag{10}$$

Since the mass matrix $\mathbf{M}_i$ is symmetric and bounded, i.e., for some $\bar{m}_i \geqslant m_i \geqslant \underline{m}_i > 0$, $\underline{m}_i\mathbf{I}_{\mathbf{n}_i} \leqslant \mathbf{M}_i \leqslant \bar{m}_i\mathbf{I}_{\mathbf{n}_i}$, it is clear that

$$\frac{\min_i\{\underline{m}_i\}}{2}\|\bar{\mathbf{s}}_i\|^2 \leqslant V(t) \leqslant \frac{\max_i\{\bar{m}_i\}}{2}\|\bar{\mathbf{s}}_i\|^2, \quad \forall\, t \geqslant 0 \tag{11}$$

Taking the time derivative of the Lyapunov function and considering Eq. (9) yields

$$\dot{V} = \sum_{i=1}^{N} \bar{\mathbf{s}}_i^T\mathbf{M}_i\dot{\bar{\mathbf{s}}}_i = -\sum_{i=1}^{N} \bar{\mathbf{s}}_i^T(\mathbf{C}_i+\mathbf{L}_i)\bar{\mathbf{s}}_i + \sum_{i=1}^{N} \{\bar{\mathbf{s}}_i^T[-\mathbf{Y}_i\theta_i - \mathbf{z}_i - \mathbf{d}_i + \mathbf{w}_i]\} \tag{12}$$

According to Tang et al. (2000), there exist constants $a_1, a_2 \geqslant 0$ such that

$$\|\dot{\mathbf{x}}_i\| \leqslant a_1\|\mathbf{x}_i\| + a_2 \tag{13}$$

If $\lambda_m(\mathbf{A})$ denotes the minimum eigenvalue of matrix $\mathbf{A}$, for sufficiently large $\lambda_m(\Lambda_i)$, i.e., $\lambda_m(\Lambda_i) > a_1$, it is possible to find Δ_{ij} such that the generalized force, i.e., $-\mathbf{Y}_i\theta_i - \mathbf{z}_i(\mathbf{x},\dot{\mathbf{x}}) - \mathbf{d}_i$ is bounded as (Tang et al. 2000)

$$\|-\mathbf{Y}_i\theta_i-\mathbf{z}_i(\mathbf{x},\dot{\mathbf{x}})-\mathbf{d}_i\|\leqslant\sum_{j=1}^{N}\{\Delta_{ij}S_j\},\quad S_j\triangleq 1+\|\bar{\mathbf{s}}_j\|+\cdots+\|\bar{\mathbf{s}}_j\|^P \tag{14}$$

Eq. (14) implies that for every subsystem, the input (including excitation and interconnections) is bounded. If the upper bound is considered in controller design, the global stability of the system can be ensured. As the upper bound can be represented using only local states, it is possible to design local controllers to achieve desired global performance.

Let δ be defined as

$$\delta\triangleq N\max_{i,j}\{\Delta_{ij}\} \tag{15}$$

Thus δS_i represents largest possible load to the ith subsystem—the worst case scenario.

Using Eqs. (14) and (15), and expression $\Sigma_{i=1}^{N}\|\bar{\mathbf{s}}_i\|\Sigma_{j=1}^{N}S_j\leqslant N\Sigma_{i=1}^{N}\|\bar{\mathbf{s}}_i\|S_i$, the second term of the right-hand side of Eq. (12) is bounded by

$$\begin{aligned}\sum_{i=1}^{N}\{\bar{\mathbf{s}}_i^T[-\mathbf{Y}_i\theta_i-\mathbf{z}_i-\mathbf{d}_i+\mathbf{w}_i]\}&\leqslant\sum_{i=1}^{N}\{\bar{\mathbf{s}}_i^T\mathbf{w}_i+\|\bar{\mathbf{s}}_i\|\|-\mathbf{Y}_i\theta_i-\mathbf{z}_i-\mathbf{d}_i\|\}\\&\leqslant\sum_{i=1}^{N}\left\{\bar{\mathbf{s}}_i^T\mathbf{w}_i+\|\bar{\mathbf{s}}_i\|\sum_{j=1}^{N}\Delta_{ij}S_j\right\}\\&\leqslant\sum_{i=1}^{N}\{\bar{\mathbf{s}}_i^T\mathbf{w}_i+\delta S_i\|\bar{\mathbf{s}}_i\|\}\end{aligned} \tag{16}$$

If the nonlinear local feedback is selected as

$$\mathbf{w}_i(\bar{\mathbf{s}}_i)=-(\delta S_i)^2\frac{\bar{\mathbf{s}}_i}{\delta S_i\|\bar{\mathbf{s}}_i\|+\varepsilon_i}\quad(\varepsilon_i>0) \tag{17}$$

then

$$\sum_{i=1}^{N}\{\bar{\mathbf{s}}_i^T[-\mathbf{Y}_i\theta_i-\mathbf{z}_i-\mathbf{d}_i+\mathbf{w}_i]\}\leqslant\sum_{i=1}^{N}\{\bar{\mathbf{s}}_i^T\mathbf{w}_i+\delta S_i\|\bar{\mathbf{s}}_i\|\}\leqslant\sum_{i=1}^{N}\varepsilon_i=\varepsilon \tag{18}$$

Furthermore, considering that the damping matrix $\mathbf{C}_i$ is positive-definite and for some $\underline{c}_i>0$, $\underline{c}_i\mathbf{I}_{\mathbf{n}_i}\leqslant\mathbf{C}_i=\mathbf{C}_i^T$, the following relationship can be obtained:

$$\begin{aligned}\dot{V}&\leqslant-\sum_{i=1}^{N}\{\bar{\mathbf{s}}_i^T(\mathbf{C}_i+\mathbf{L}_i)\bar{\mathbf{s}}_i\}+\varepsilon\\&\leqslant-\min_i\{\alpha_i\}\sum_{i=1}^{N}\bar{\mathbf{s}}_i^T\mathbf{M}_i\bar{\mathbf{s}}_i+\varepsilon\leqslant-2\alpha V+\varepsilon\end{aligned}$$

$$\alpha_i\triangleq\frac{\lambda_m\{\underline{c}_i\mathbf{I}_{\mathbf{n}_i}+\mathbf{L}_i\}}{\bar{m}_i},\quad\alpha\triangleq\min_i\{\alpha_i\} \tag{19}$$

Expression (19) implies

$$V(t)\leqslant\left[V\left(t_0-\frac{\varepsilon}{2\alpha}\right)\right]e^{-2\alpha(t-t_0)}+\frac{\varepsilon}{2\alpha} \tag{20}$$

Thus, the closed-loop system (9) is globally stable in the sense that all signals are uniformly bounded by

$$\|\bar{\mathbf{s}}(t)\|^2\leqslant m_{\mathbf{r}}\left\{\|\bar{\mathbf{s}}(t_0)\|^2-\frac{\varepsilon}{\alpha\max_i\{\bar{m}_i\}}\right\}e^{-2\alpha(t-t_0)}+m_{\mathbf{r}}\frac{\varepsilon}{\underline{\lambda}_m\{\underline{c}_i\mathbf{I}_{\mathbf{n}_i}+\mathbf{L}_i\}} \tag{21}$$

where $\|\bar{\mathbf{s}}(t)\|^2=\Sigma\|\bar{\mathbf{s}}_i\|^2$, $m_{\mathbf{r}}\triangleq\max_i\{\bar{m}_i\}/\min_i\{\underline{m}_i\}$, and for some set of matrices $\mathbf{T}_1,\mathbf{T}_2,\ldots,\mathbf{T}_N$—where the set is denoted $\{\mathbf{T}_i\}$ for short—the notation $\underline{\lambda}_m(\{\mathbf{T}_i\})$ is defined to be $\min_i\{\lambda_m(\mathbf{T}_i)\}$; $\bar{m}_i$ and $\underline{m}_i$ =upper and lower bounds of the masses in substructure i, respectively, hence $m_{\mathbf{r}}\geqslant 1$ is a measure of the level of unevenness of mass distribution of the system. Using Eqs. (21) and (7), the norms of the displacements converge to

$$\|\mathbf{x}_i\|^2\leqslant m_{\mathbf{r}}\frac{\varepsilon}{\underline{\lambda}_m^2(\Lambda_i)\underline{\lambda}_m\{\underline{c}_i\mathbf{I}_{\mathbf{n}_i}+\mathbf{L}_i\}} \tag{22}$$

As seen in the above derivation, the local stability of the controller is achieved through proper design of the linear feedback gain $\mathbf{L}_i$. As there is no communication or information exchange among the subsystems, the global stability of the controller is ensured by using an ultimate upper bound of the combined effect of excitation and interconnections for all subsystems [see Eqs. (14) and (15)]. This upper bound represents the largest possible external load of the subsystems and every local controller is designed against such worst scenario using a nonlinear feedback term as defined in Eq. (17). Therefore, desired global system behavior may be achieved. Note that in the previous method (Ma et al. 2008) $\eta_i\triangleq\mathbf{Y}_i\theta_i$ is included such that the control law is

$$\mathbf{u}_i=\eta_i-\mathbf{L}_i\bar{\mathbf{s}}_i+\mathbf{w}_i \tag{23}$$

In this case, the right-hand-side of Eq. (9) becomes $-\mathbf{z}_i(\mathbf{x}_i,\dot{\mathbf{x}}_i)-\mathbf{d}_i+\mathbf{w}_i$, which generally results in a smaller upper bound δ and thus smaller control force. The benefit of removing η_i is that the control force can be determined without precise information about the structural parameters. The controller may be more robust and more suitable for applications of complex structures.

Performance Analysis

The system equation of the ith subsystem (5) can be written as

$$\dot{\xi}_i=\mathbf{A}_i\xi_i+\mathbf{B}_i\mathbf{u}_i-\mathbf{z}_i(\mathbf{x}_i,\dot{\mathbf{x}}_i)-\mathbf{d}_i \tag{24}$$

with

$$\xi_i=\begin{bmatrix}\mathbf{x}_i\\\dot{\mathbf{x}}_i\end{bmatrix},\quad\mathbf{A}_i\triangleq\begin{bmatrix}\mathbf{0}_{\mathbf{n}_i}&\mathbf{I}_{\mathbf{n}_i}\\-\mathbf{M}_i^{-1}\mathbf{K}_i&-\mathbf{M}_i^{-1}\mathbf{C}_i\end{bmatrix}$$

$$\mathbf{B}_i\triangleq\begin{bmatrix}\mathbf{0}_{\mathbf{n}_i}\\\mathbf{M}_i^{-1}\mathbf{B}_{0i}\end{bmatrix}$$

The sliding mode variable may thus be written as $\bar{\mathbf{s}}_i=\mathbf{Q}_i\xi_i$ with $\mathbf{Q}_i=\text{blockdiag}[\Lambda_i\ \mathbf{I}_{\mathbf{n}_i}]$. A block diagram of the subsystem is shown in Fig. 1. It is seen that in this case there appears a new feedback channel with a gain of $\mathbf{M}_i\Lambda_i s+\mathbf{C}_i\Lambda_i-\mathbf{K}_i$ from output $[\mathbf{x}_i(t)]$ directly to input $[-\mathbf{d}_i-\mathbf{z}_i(\mathbf{x}_i,\dot{\mathbf{x}}_i)]$ as compared to the previous method [see Fig. 2 in Ma et al. (2008)]. Note that while $\mathbf{z}_i(\mathbf{x}_i,\dot{\mathbf{x}}_i)$ is part of the dynamics of the system, it may be treated as an input to the ith subsystem if only the local dynamics of subsystem are of concern.

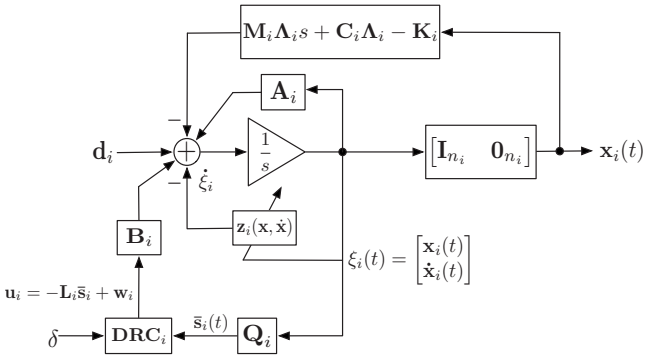

Fig. 1. Block diagram of a structure controlled by the present method

Case 1

$\delta S_i\|\bar{\mathbf{s}}_i\| \to \delta\|\bar{\mathbf{s}}_i\|^{p+1} \gg \varepsilon_i$ for relatively large $\|\bar{\mathbf{s}}_i\|$. In this case, the nonlinear compensation term, $\mathbf{w}_i$ simplifies to

$$\mathbf{w}_i = -\delta S_i \frac{\bar{\mathbf{s}}_i/\|\bar{\mathbf{s}}_i\|}{1+\varepsilon_i/(\delta S_i\|\bar{\mathbf{s}}_i\|)} \approx -\delta S_i\left(1-\frac{\varepsilon_i}{\delta S_i\|\bar{\mathbf{s}}_i\|}\right)\frac{\bar{\mathbf{s}}_i}{\|\bar{\mathbf{s}}_i\|} \tag{25}$$

Thus

$$\mathbf{M}_i\dot{\bar{\mathbf{s}}}_i + [\mathbf{C}_i+\mathbf{L}_i]\bar{\mathbf{s}}_i \approx -\delta S_i\left(1-\frac{\varepsilon_i}{\delta S_i\|\bar{\mathbf{s}}_i\|}\right)\frac{\bar{\mathbf{s}}_i}{\|\bar{\mathbf{s}}_i\|} - \mathbf{Y}_i\theta_i - \mathbf{z}_i(\mathbf{x},\dot{\mathbf{x}}) - \mathbf{d}_i \tag{26}$$

A block diagram of the ith subsystem with simplified system Eq. (26) is shown in Fig. 2(a).

In this case, the control force vector can be determined as

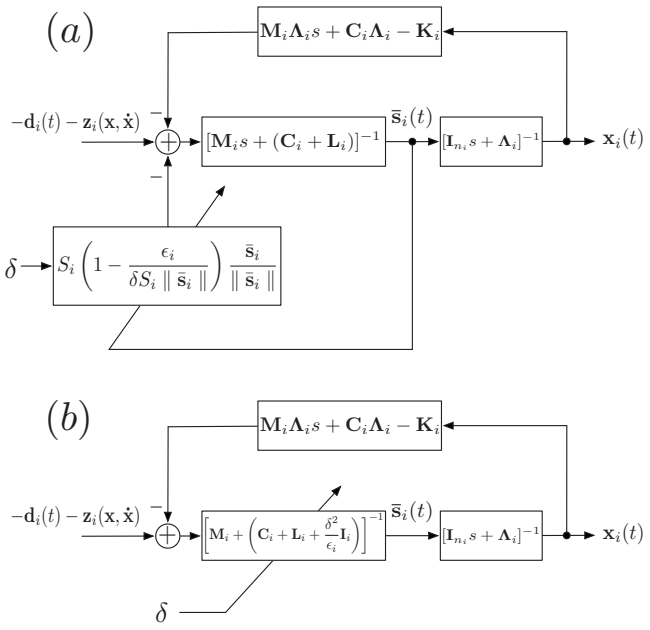

Fig. 2. Block diagram of equivalent systems for (a) $\delta S_i\|\bar{\mathbf{s}}_i\| \gg \varepsilon_i$; (b) $\delta S_i\|\bar{\mathbf{s}}_i\| \ll \varepsilon_i$

$$\mathbf{u}_i \approx -\left[\mathbf{L}_i + \left(1-\frac{\varepsilon_i}{\delta S_i\|\bar{\mathbf{s}}_i\|}\right)\frac{\delta S_i}{\|\bar{\mathbf{s}}_i\|}\mathbf{I}_{\mathbf{n}_i}\right]\bar{\mathbf{s}}_i \approx -\mathbf{L}_i\bar{\mathbf{s}}_i - (\delta\|\bar{\mathbf{s}}_i\|^p)\bar{\mathbf{s}}_i \tag{27}$$

Eqs. (7) and (27) imply that the linear feedback channel ($\mathbf{L}_i$) provides additional passive viscous damping and passive linear stiffness to the system, whereas the role of the nonlinear portion of the control force ($\mathbf{w}_i$) is somewhat similar to that of additional nonlinear damping and nonlinear elastic stiffness. For a subsystem that includes only one floor level and $p=2$, $\omega_i \approx -\delta\bar{s}_i^3$. Note that large $\|\bar{\mathbf{s}}_i\|$ corresponds to large structural response, which may be due to strong excitations and/or ineffective control performance.

Case 2

$\|\bar{\mathbf{s}}_i\| \to 0^+$ and hence $\delta S_i\|\bar{\mathbf{s}}_i\| \to \delta\|\bar{\mathbf{s}}_i\| \ll \varepsilon_i$. Eq. (17) simplifies to

$$\mathrm{w}_i = -\frac{\delta^2}{\varepsilon_i}S_i^2\frac{\bar{\mathbf{s}}_i}{1+\dfrac{\delta S_i\|\bar{\mathbf{s}}_i\|}{\varepsilon_i}} \overset{\|\bar{\mathbf{s}}_i\|\to 0}{\to} -\frac{\delta^2}{\varepsilon_i}\bar{\mathbf{s}}_i \tag{28}$$

The system equations of the ith subsystem can thus be written as

$$\mathbf{M}_i\dot{\bar{\mathbf{s}}}_i + \left(\mathbf{C}_i + \mathbf{L}_i + \frac{\delta^2}{\varepsilon_i}\mathbf{I}_{\mathbf{n}_i}\right)\bar{\mathbf{s}}_i \approx -\mathbf{Y}_i\theta_i - \mathbf{z}_i(\mathbf{x},\dot{\mathbf{x}}) - \mathbf{d}_i \tag{29}$$

The system can be approximately treated as a linear system. A block diagram of the approximate linear system is given in Fig. 2(b). The closed-loop transfer function from the input $[-\mathbf{d}_i - \mathbf{z}_i(\mathbf{x},\dot{\mathbf{x}})]$ to output $\mathbf{x}_i(t)$ can be obtained as

$$\mathbf{G}_i(s) = \left\{\mathbf{M}_i s^2 + \left(2\mathbf{M}_i\Lambda_i + \mathbf{C}_i + \mathbf{L}_i + \frac{\delta^2}{\varepsilon_i}\mathbf{I}_{\mathbf{n}_i}\right)s + \left[\left(2\mathbf{C}_i + \mathbf{L}_i + \frac{\delta^2}{\varepsilon_i}\mathbf{I}_{\mathbf{n}_i}\right)\Lambda_i - \mathbf{K}_i\right]\right\}^{-1} \tag{30}$$

In order to ensure that the above closed-loop subsystem is stable, $\mathbf{G}_i$ must not have poles on the right-hand complex plane, i.e., none of the roots of Eq. (31) has positive real part. This condition implies that matrices $\mathbf{M}_i$, $2\mathbf{M}_i\Lambda_i + \mathbf{C}_i + \mathbf{L}_i + (\delta^2/\varepsilon_i)\mathbf{I}_{\mathbf{n}_i}$, and $[2\mathbf{C}_i + \mathbf{L}_i + (\delta^2/\varepsilon_i)\mathbf{I}_{\mathbf{n}_i}]\Lambda_i - \mathbf{K}_i$ must be positive-definite.

$$\left|\mathbf{M}_i s^2 + \left(2\mathbf{M}_i\Lambda_i + \mathbf{C}_i + \mathbf{L}_i + \frac{\delta^2}{\varepsilon_i}\mathbf{I}_{\mathbf{n}_i}\right)s + \left[\left(2\mathbf{C}_i + \mathbf{L}_i + \frac{\delta^2}{\varepsilon_i}\mathbf{I}_{\mathbf{n}_i}\right)\Lambda_i - \mathbf{K}_i\right]\right| = 0 \tag{31}$$

Since $\mathbf{M}_i$, $\mathbf{C}_i$, and $\mathbf{K}_i$ are positive-definite for a structure, for any positive-definite (or positive semidefinite) $\mathbf{L}_i$, a sufficient condition for stability is that $[2\mathbf{C}_i + \mathbf{L}_i + (\delta^2/\varepsilon_i)\mathbf{I}_{\mathbf{n}_i}]\Lambda_i - \mathbf{K}_i$ is positive-definite. Thus, a controller may be designed so that

$$\frac{\delta^2}{\varepsilon_i}\Lambda_i - \mathbf{K}_i \geq 0 \ \text{ and } \ \mathbf{L}_i \geq 0, \ \text{ or } \ \mathbf{L}_i \approx \mathbf{K}_i\Lambda_i^{-1} \ \text{ and } \ \frac{\delta^2}{\varepsilon_i} > 0 \tag{32}$$

Note that $\mathbf{A}-\mathbf{B} \geq 0$ means $\mathbf{A}-\mathbf{B}$ is positive semidefinite. A design with relatively large stability margin may be chosen as

$$\mathbf{L}_i \approx \mathbf{K}_i\Lambda_i^{-1} \ \text{ and } \ \frac{\delta^2}{\varepsilon_i}\mathbf{I}_{\mathbf{n}_i} > \mathbf{K}_i\Lambda_i^{-1} \tag{33}$$

Under such a design, control force can be estimated as

$$\mathbf{u}_i \approx -\left(\mathbf{L}_i + \frac{\delta^2}{\varepsilon_i}\mathbf{I}_{\mathbf{n}_i}\right)\bar{\mathbf{s}}_i = -\left(\mathbf{L}_i + \frac{\delta^2}{\varepsilon_i}\mathbf{I}_{\mathbf{n}_i}\right)(\dot{\mathbf{x}}_i + \Lambda_i \mathbf{x}_i) \tag{34}$$

In this case, the controller simply provides additional passive viscous damping and passive linear stiffness to the system.

It is interesting to note that for both cases, the controllers provide additional passive viscous damping and passive linear stiffness. In Case 1 particularly, the controllers also provide additional nonlinear damping and nonlinear elastic stiffness. If $\mathbf{x}_i$ is defined as interstory drift, the additional damping and stiffness are essentially passive *internal* damping and interstory stiffness, respectively, whereas if $\mathbf{x}_i$ is defined as displacement relative to the ground, the controllers generate additional passive *external* damping and passive stiffness relative to ground. The former case results in a *stronger* structure whereas the latter is similar to the case where additional *global supports* from the ground are provided.

The two special cases represent the two extreme conditions. The actual closed-loop system behavior may be located somewhere in-between these two cases. Depending on the selection of controller parameters, i.e. Λ_i, $\mathbf{L}_i$, ε_i, and δ, as well as the level of excitation, the behavior of the resultant closed-loop system may be closer to that in either case. Generally, system behavior closer to Case 2 may be more favorable as it corresponds to small structural responses. Note that while a controller designed using Eq. (33) may offer good performance in response reduction due to its large feedback gains, it may also demand large control forces, which may become a problem when the capacity of the actuators are limited.

Estimate of Control Force Level

According to the bound of the sliding mode variable (21), the magnitude of the control forces can be estimated using Eq. (8) so that the controllers may be designed according to realistic factors such as the capacity of the actuators to be used, maximum allowable structural responses, etc. To illustrate this process, let $\|\bar{\mathbf{s}}(0)\|=0$ for simplicity. The control force of the jth floor in the ith subsystem is then bounded as

$$\|u_{ij}(t)\| \leq \left(\bar{l}_i + \frac{(\delta S_i)^2}{\delta S_i \|\bar{\mathbf{s}}_\mathbf{i}\| + \varepsilon_i}\right)\|\bar{\mathbf{s}}\|, \quad i = 1,2,\ldots,N, \quad j = 1,2,\ldots,\mathbf{n}_i \tag{35}$$

where $\bar{l}_i$=maximum eigenvalue of $\mathbf{L}_i$. For a proper control design, $\|\bar{\mathbf{s}}(t)\|^2 \leq m_\mathbf{r} N \bar{\varepsilon}_i/(\underline{c}_i+\underline{l}_i)$ [see Eq. (21)], where an overbar and an underbar represent the maximum and minimum values, respectively. If the parameters are selected such that $\delta^2/\bar{\varepsilon}_i = \rho_i \bar{l}_i$, it can be shown that the control force is bounded as

$$\|u_{ij}(t)\| \leq (\sqrt{m_\mathbf{r} N \rho_i \mu_i} + 1 + \Psi + \Psi^2)\delta, \quad \mu_i \triangleq \frac{\bar{l}}{\underline{c}_i + \underline{l}_i}$$
$$\Psi \triangleq \sqrt{\frac{m_\mathbf{r} N \bar{\varepsilon}_i}{\underline{c}_i + \underline{l}_i}} \tag{36}$$

In this study, $\Psi < 1$ and the same parameters are used for the local controllers, thus $\rho_i = 1$ and $\mu_i < 1$. The bound of peak control force becomes

$$\|\mu_{ij}(t)\| \leq (\sqrt{m_\mathbf{r} N} + 3)\delta \tag{37}$$

Eqs. (36) and (37) suggest that the peak control force may increase monotonically with the level of unevenness in structural mass distribution, the level of decentralization (indicated by N) and the strength of the excitation [indicated by δ; see Eqs. (14) and (15)]. For a given structure, $m_\mathbf{r}$ is fixed. If the capacity of the actuators to be used is of primary concern, smaller number of subsystem and lower δ should be used. Note that when $N=1$, the control scheme becomes a centralized one. Selecting a smaller value of δ may lower the bound of peak control force; however, excessively small δ may cause the condition for convergence to be violated [see Eqs. (14) and (15)]. In such a case, Eqs. (36) and (37) are invalid. The resultant controller may still stabilize the structure if $2\mathbf{M}_i\Lambda_i + \mathbf{C}_i + \mathbf{L}_i + (\delta^2/\varepsilon_i)\mathbf{I}_{\mathbf{n}_i}$ and $[2\mathbf{C}_i + \mathbf{L}_i + (\delta^2/\varepsilon_i)\mathbf{I}_{\mathbf{n}_i}]\Lambda_i - \mathbf{K}_i$ are positive-definite [see Eq. (30)], however, the level of control force required may still be high.

Selection of Λ_i

In order to achieve the desired control performance as defined in Eqs. (22) and (36), the minimum eigenvalue of Λ_i should be greater than a_1, defined in Eq. (13). Due to the uncertainties in the system, precisely determining a_1 can be difficult. However it can be estimated using the modal properties of the structure.

The structural response due to an earthquake can be written as

$$\begin{cases} x_i(t) = A_0 + A_1 \cos(\omega_1 t + \phi_1) + A_2 \cos(\omega_2 t + \phi_2) + \cdots \\ \dot{x}_i(t) = A_1\omega_1 \sin(\omega_1 t + \phi_1) + A_2\omega_2 \sin(\omega_2 t + \phi_2) + \cdots \end{cases} \tag{38}$$

In the case where the first vibration mode dominates, the amplitudes of $x_i(t)$ and $\dot{x}_i(t)$ are approximately A_1 and $A_1\omega_1$, respectively. Thus, Λ_i may be selected such that its smallest eigenvalue is greater than the frequency of the first vibration mode ω_1. Λ_i may also be selected following the procedure based on an optimization process (Ma et al. 2008), i.e., $\Lambda_i = \sqrt{\gamma_i \mathbf{M}_i^{-1}\mathbf{K}_i}$, where $\gamma_i > 0$ is a weighting factor.

Illustrative Examples

In order to evaluate and assess the performance of the proposed method, three models are chosen as illustrative examples for this study. They are an eight-story shear beam model (Ma et al. 2005; Spencer et al. 1994; Yang 1982), a two-story nonlinear shear beam model (Yang and Lin 2005), and a 20-story elastic benchmark model (Spencer et al. 1998a). In these examples, sensor noise, sensor and actuator dynamics are not considered. Actuators are assumed to be installed using chevron braces.

Example 1: Eight-Story Shear Beam Model

An eight-story shear beam model is considered first. The mass, stiffness, and damping coefficient for every floor are assumed to be $m=3.456\times10^5$ kg, $c=2.4\times10^6$ N·s/m, and $k=3.404\times10^8$ N/m, respectively. The first three natural frequencies of the model are 5.79, 17.18, and 27.98 rad/s, respectively; the corresponding damping ratios are 2, 6, and 10%, respectively. This model is decomposed into eight subsystems, every story being a subsystem. Actuators are assumed to be installed between adjacent stories to provide control forces for every floor. The

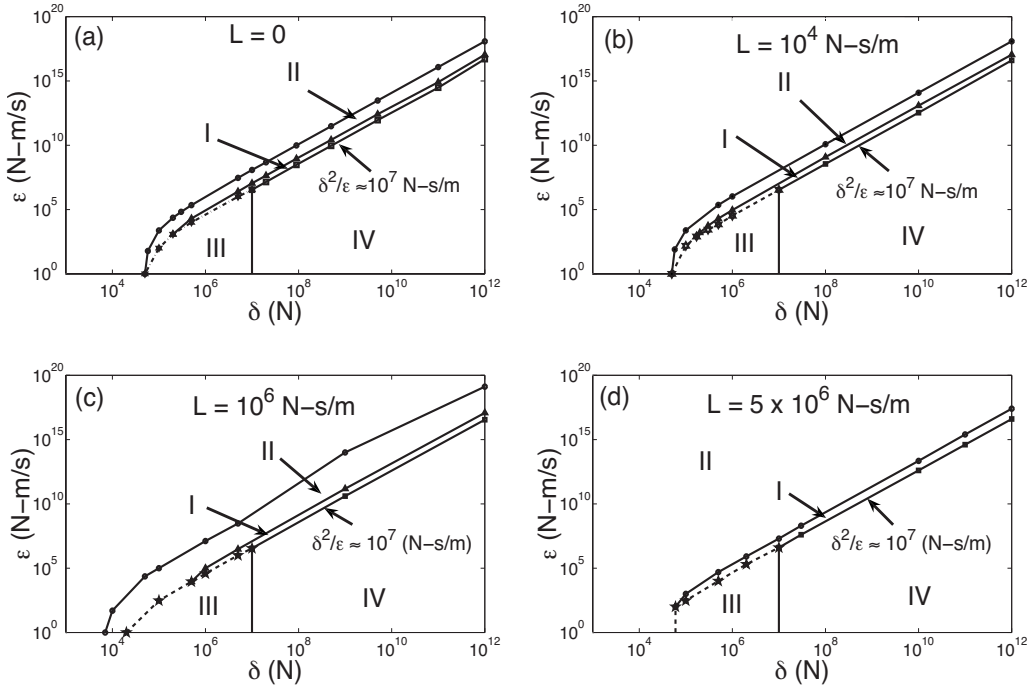

Fig. 3. Convergence regions of the present method for $L=0-5\times10^6$ N·s/m (I—optimal region: percentage reduction ⩾98.5%, II—suboptimal region: percentage reduction ⩾75%, III—chattering region, and IV—undesired control performance region) $\Lambda=31.38$ rad/s for all cases

sliding mode variable is defined based on the displacement relative to the ground. The same controller design is used for all subsystems. Thus the control parameters are the same for every subsystem and they are denoted as L, Λ, and ε—the subscript i is dropped hereafter.

The control performance is first studied using the *N-S* component of ground acceleration from the 1940 El Centro earthquake under different values of linear feedback gain L. Namely, L is selected between 0 and 3×10^7 N·s/m. The earthquake is scaled so that the peak ground acceleration is 0.35 m/s^2 in order to be consistent with the previous study. $\Lambda=\sqrt{\text{km}}=31.38$ rad/s is selected ($\gamma_i=1$) (Ma et al. 2008). The regions, within which the ultimate bound of the parameter uncertainty δ and the design parameter ε can be freely selected to achieve the same control performance, are obtained for every value of L selected through

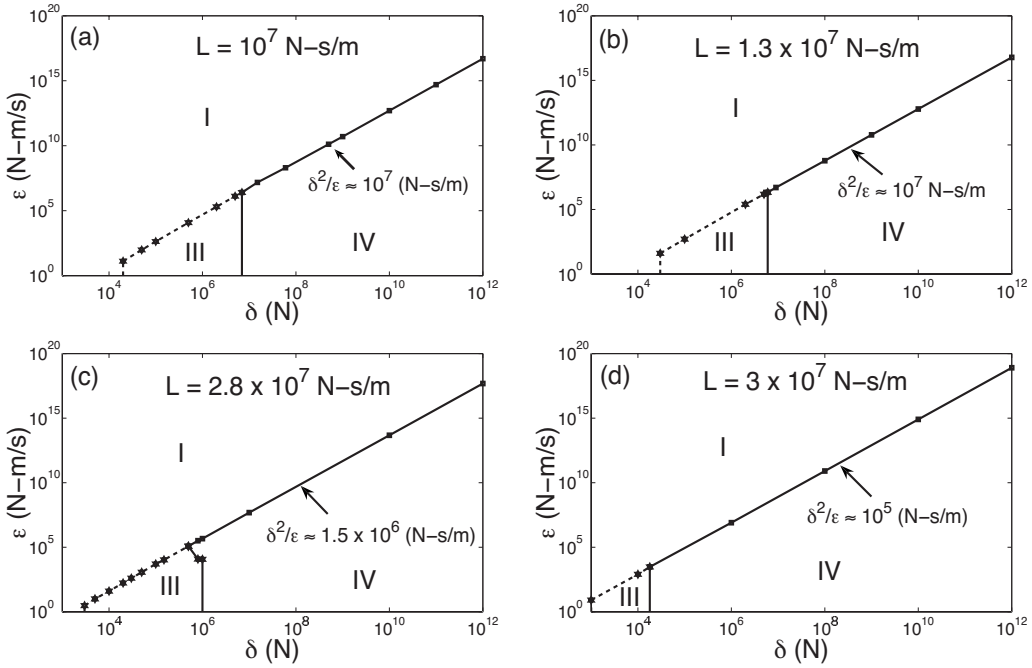

Fig. 4. Convergence regions of the present method for $L=1-3\times10^7$ N·s/m (regions defined the same as in Fig. 3)

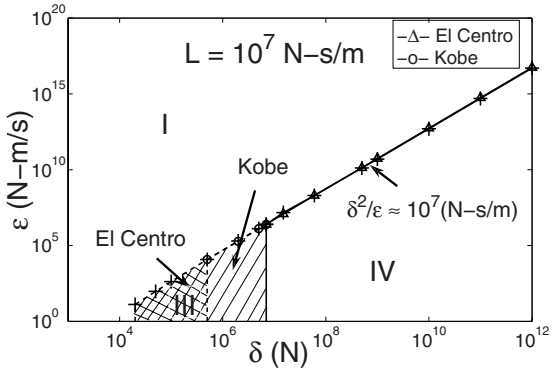

Fig. 5. Convergence regions of the eight-story shear beam model excited by the 1940 El Centro and the 1995 Kobe earthquakes (regions defined as in Fig. 3)

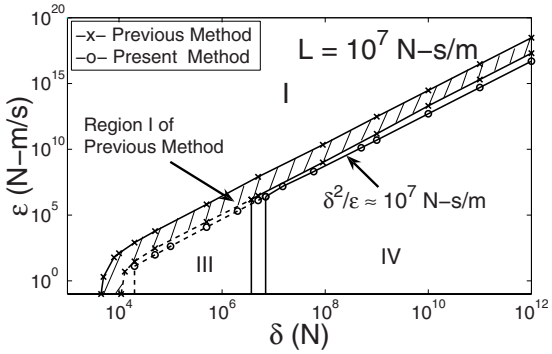

Fig. 6. Convergence regions of the previous and present methods (regions defined as in Fig. 3)

extensive simulations. These regions are shown in Figs. 3 and 4 for $L=0-5\times10^6$ N·s/m and $L=10^7-3\times10^7$ N·s/m, respectively. For this example, it is seen that the region of effective control performance and the region of undesired control performance are clearly separated by an almost straight line in the logarithmic scale. Specifically, as shown in Figs. 3(a–c), for $L=0-10^6$ N·s/m, two regions of effective control performance are identified, which are named as the suboptimal convergence region and optimal convergence region. In the suboptimal convergence region, the percent reduction in the maximum interstory drift (occurring on the first floor in this example) is greater than 75%, while in the optimal convergence region, greater than 98.5% reduction can be achieved. When L is relatively small, i.e., $L=0-10^4$ N·s/m, both regions are restricted within the two narrow bands above a boundary described by $\delta^2/\varepsilon\approx10^7$ (N·s/m) and $\delta>2\times10^4$ N, as indicated by Eqs. (15) and (33). As L increases to 10^6 N·s/m, the suboptimal region expands substantially [see Fig. 3(c)]. When L reaches 5×10^6 N·s/m, there is no longer an upper limit on this region as shown in Fig. 3(d). In Fig. 4(a), it is shown that as L reaches 10^7 N·s/m ($\approx\sqrt{\text{km}}$), the two regions merge into one and the optimal region falls above the boundary line defined by $\delta^2/\varepsilon\approx10^7$ (N·s/m). Further increasing L allows for a smaller value of δ to be used and when $L\geqslant3\times10^7$ N·s/m there is no lower limit on the value of δ for convergence purpose. It is noted that all the plots in Figs. 3 and 4 are limited by $\varepsilon=10^{20}$ N·m/s and $\delta=10^{12}$ N. The region beyond these values may not be necessary or practical for controller design as these limits far exceed the values of the capacity of typical large-scale actuators. In this study, the performance of the present method is thus evaluated within the region confined by these limits. The proposed method is essentially a sliding mode control method. When the parameters are not selected properly, it may have the problem of chattering as does a typical sliding mode method. In this example, controllers designed with smaller values of δ and ε are more sensitive to such problem. The regions of chattering are identified and shown also in Figs. 3 and 4.

The *E-W* component of ground acceleration of the 1995 Kobe earthquake is also considered in this example. The regions of control performance obtained are shown in Fig. 5 for $L=10^7$ N·s/m. It is seen that the regions of the two earthquakes almost overlap completely except that for the Kobe earthquake, a larger value of δ (approximately 5×10^5 N as opposed to approximately 2×10^4 N for the El Centro earthquake) is required to avoid chattering. This is due, in part to the fact that the ground accelerations of Kobe earthquake have much larger crests and troughs as compared to those of the scaled El Centro earthquake.

Fig. 6 shows the comparison between these regions of the previous method (Ma et al. 2008) and the present method for $L=10^7$ N·s/m under the El Centro earthquake. It is seen that the optimal region of the previous method is confined within a narrow band, whereas that of the present method covers the entire half-plane over the boundary defined by $\delta^2/\varepsilon=10^7$ N·s/m. Controllers can thus be designed with greater flexibility using the present method.

Table 1 summarizes the results of the two methods for the scaled El Centro earthquake with the following controller parameters: $\Lambda=31.38$ rad/s, $L=10^7$ N·s/m, $\delta=10^6$ N, and $\varepsilon=10^6$ N·m/s. As a comparison, a passively controlled case where significant passive damping is added to the structure is considered. More specifically, additional viscous damping of 8.4×10^6 N·s/m is added to every floor such that the damping ratios of the first three modes are 9.19, 27.25, and 44.38%, respectively. Damping ratios of the higher modes are much larger, approaching 100%. The results of the three cases are normalized against those of the uncontrolled case—the values shown in the table represent the ratios between the results of the controlled and uncontrolled cases. Moreover, the numbers on the top of every cell refer to the peak values and those on the bottom refer to the root-mean-square (RMS) values. Note that the control force at a single floor is not the same as that provided by the actuators on the same floor. The forces requested from the actuators are determined using Eq. (4) with $\chi_i=1$. It is seen that the structural displacements (relative to ground) and interstory drifts are more significantly reduced by the two active control methods as compared to the passively controlled case. The present method, achieves the most reduction in displacements and drifts, however, as compared to the previous method, it requires larger control forces, resulting in larger accelerations.

The robustness of the present method with regard to structural parameter uncertainty is then evaluated. The masses of the second, fourth, sixth, and eighth floor are assumed to be twice as large as their original values, i.e., $m_2=m_4=m_6=m_8=6.912\times10^5$ kg and the stiffness coefficients of the corresponding floors are assumed to be reduced by 50%, i.e., $k_2=k_4=k_6=k_8=1.702\times10^8$ N/m. The controllers are first designed using both methods assuming that the changes are unknown to the designer. The same parameters are selected for the two controllers: $\Lambda=31.38$ rad/s, $L=10^7$ N·s/m, $\delta=10^6$ N, and $\varepsilon=10^6$ N·m/s. When the controllers are applied to the structure, the unchanged values of mass and stiffness, i.e., $m=3.456\times10^5$ kg and $k=3.404\times10^8$ N/m are

Table 1. Performance of Passive, Previous (Method I), and Present (Method II) Methods under the Scaled 1940 El Centro Earthquake (Peak Values Stacked on Top of RMS Values)

Floor level	1st	2nd	3rd	4th	5th	6th	7th	8th
				Displacement relative to ground (percentage of uncontrolled)				
Passive	62.11	60.99	60.02	59.28	58.53	57.65	57.03	56.80
	44.59	44.56	44.58	44.62	44.66	44.70	44.72	44.73
Method I	8.69	6.26	4.82	3.78	3.14	2.75	2.53	2.44
	4.18	3.19	2.43	2.09	1.77	1.57	1.46	1.41
Method II	6.25	4.36	3.25	2.59	2.18	1.92	1.77	1.70
	3.14	2.24	1.71	1.38	1.18	1.05	0.98	0.95
				Interstory drift (percentage of uncontrolled)				
Passive	62.11	60.17	58.88	56.83	54.26	52.57	50.81	50.00
	44.59	44.59	44.72	44.90	45.04	45.09	45.04	44.94
Method I	8.69	4.37	2.11	0.96	0.71	0.43	0.42	0.38
	4.18	2.17	1.55	0.87	0.77	0.54	0.43	0.22
Method II	6.25	2.67	1.30	0.62	0.32	0.18	0.11	0.09
	3.14	1.37	0.63	0.31	0.16	0.10	0.07	0.06
				Absolute acceleration (percentage of uncontrolled)				
Passive	88.91	57.53	57.92	62.30	62.18	57.17	53.33	51.72
	73.63	55.03	46.23	45.52	45.54	45.17	45.55	45.91
Method I	120.00	84.09	75.51	72.00	65.45	54.55	46.15	42.35
	87.50	63.64	46.67	38.89	33.33	29.17	26.92	25.92
Method II	129.44	107.52	94.34	89.18	79.88	66.29	56.04	51.41
	101.65	80.62	60.03	49.72	42.31	36.88	33.99	32.72
				Control force (kN)				
Method I	103	112	116	122	124	125	125	125
	16	22	24	25	25	25	25	25
Method II	100	143	152	153	152	152	152	152
	19	27	29	30	31	31	31	31
				Actuator force (kN)				
Method I	901	836	736	621	498	374	249	125
	185	170	148	124	99	74	49	25
Method II	1,153	1,053	910	758	605	453	302	151
	227	208	182	152	122	91	61	31

used to calculate the term η in Eq. (23) for the controller designed with the previous method. Note that the term η does not exist in the present method. The case in which the actual changed mass and stiffness, i.e., $m=6.912\times10^5$ kg and $k=1.702\times10^8$ N/m are used to calculate η is also considered. The results obtained are again normalized with respect to those of the uncontrolled case and are tabulated in Table 2. The normalized results of the passively controlled case are also included for comparison. As seen here, the active controllers reduce the structural displacements and drifts much more significantly than the passive controller, however with noticeably larger accelerations. While both active methods are shown to be robust to the parameter changes, the structural response is reduced more significantly with the present method, however with larger control forces. The robustness of the present method has also been validated by other cases with different parameter variations. The results are similar and are omitted here for simplicity of presentation. The reader is referred to a Ph.D. thesis (Johansen 2008) for a detailed presentation of these results.

It should be noted that reducing structural response has been the primary objective in controller design in the above case studies. The resultant controller is effective when the earthquake is relatively weak, as demonstrated in the case of the scaled earthquake, in which the control forces are somewhat large but are still within a realistic limit. In the case of a strong earthquake such as the full-scale 1940 El Centro earthquake, the same controller may demand significantly larger forces, e.g., more than half of the story weight (Johansen 2008), which may cause other problems in practice. In such a case, the control parameters need to be adjusted to accommodate the capacity of the actuators. For instance if the control force of every floor level is to be limited by 700 kN, the controller may be designed as follows. According to Eq. (37), the controller is designed as $\delta=1.7\times10^5$ N, $L=1.7\times10^5$ N·s/m, and $\varepsilon=1.7\times10^5$ N·m/s. Parameter $\Lambda=10$ rad/s$>\omega_1=5.79$ rad/s is selected. The controller results in peak displacement (relative to ground) of 94.8 mm on the roof, peak interstory drift of 17.93 mm at the first floor, and peak acceleration of 0.56 g on the roof. The largest control force is on the roof, 691 kN, which is about 20%

Table 2. Comparison of Performance of Passive, Previous, and Present Methods with regard to Uncertainty in Structural Parameters (Method IA: Previous Method without Knowledge of Uncertainties, Method IB: Previous Method with Knowledge of Uncertainties, and Method II: Present Method) (Peak Values Stacked on Top of RMS Values)

Floor level	1st	2nd	3rd	4th	5th	6th	7th	8th
				Displacement relative to ground (percentage of uncontrolled)				
Passive	54.84	53.65	54.76	56.23	57.55	58.80	59.58	60.38
	55.51	54.60	54.74	54.61	54.86	54.69	54.72	54.61
Method IA	12.27	9.11	6.76	5.74	4.52	4.44	3.80	4.56
	6.86	5.00	3.85	3.06	2.57	2.44	2.19	2.42
Method IB	10.83	6.40	5.31	3.92	3.63	3.07	3.01	2.91
	5.88	3.33	2.82	1.98	1.77	1.49	1.42	1.33
Method II	9.03	6.65	4.54	4.20	3.12	3.29	2.69	3.41
	4.90	4.00	2.56	2.34	1.77	1.76	1.42	1.81
				Interstory drift (percentage of uncontrolled)				
Passive	60.59	60.27	64.92	63.16	69.43	65.65	57.97	51.77
	55.51	54.20	55.76	54.10	55.21	52.76	52.30	49.88
Method IA	12.27	7.84	5.63	2.53	7.41	3.79	9.43	12.03
	6.86	4.02	2.22	1.76	2.86	1.61	4.88	5.26
Method IB	10.83	4.29	3.90	0.69	3.70	2.07	5.66	4.43
	5.88	2.01	2.22	0.52	1.43	0.81	2.44	1.75
Method II	9.02	6.72	4.76	3.46	8.64	4.83	12.26	12.66
	4.90	3.52	2.22	1.76	4.29	2.42	4.88	7.02
				Absolute acceleration (percentage of uncontrolled)				
Passive	88.17	67.52	60.57	45.96	51.92	60.60	67.89	56.16
	85.21	56.63	55.77	51.03	53.90	56.62	55.88	52.71
Method IA	102.86	105.71	112.50	115.63	116.67	120.00	125.00	94.87
	100.12	88.89	77.78	70.00	70.00	63.64	58.33	50.00
Method IB	102.86	105.71	115.63	115.63	123.33	123.33	132.14	94.87
	114.29	88.89	77.78	70.00	70.00	63.64	58.33	50.00
Method II	99.85	100.31	100.26	99.79	100.12	100.57	96.43	98.78
	114.29	111.11	100.00	100.21	90.00	90.91	75.00	71.43
				Control force (kN)				
Method IA	101	170	115	144	114	137	115	150
	18	37	33	40	34	40	35	44
Method IB	112	224	127	248	132	249	133	251
	18	46	27	49	28	49	28	50
Method II	103	251	198	264	203	264	210	302
	21	49	42	54	43	54	45	61
				Actuator force (kN)				
Method IA	1,398	1,323	1,153	983	787	607	407	150
	278	262	225	192	153	118	79	44
Method IB	1,423	1,262	1,139	1,013	766	633	384	251
	290	275	230	203	154	127	127	78
Method II	1,739	1,666	1,435	1,241	978	775	512	302
	364	345	297	256	202	159	105	61

of the story weight. As a comparison, the passive controller results in peak displacement of 114.32 mm, peak interstory drift of 21.03 mm, and peak acceleration of 0.44 g. The maximum floor force from the dampers is 863 kN at the first floor, about 25% of the story weight.

Two-Story Nonlinear Elastic Shear Beam Model

A two-story nonlinear elastic shear beam model is chosen as the second example. The governing equations of the model are (Yang and Lin 2005)

$$\begin{cases} m_1\ddot{x}_1 + c_1\dot{x}_1 - c_2\dot{x}_2 + k_{11}x_1 + k_{13}x_1^3 - k_{21}x_2 - k_{23}x_2^3 = -m_1\ddot{x}_g + u_1 \\ m_2(\ddot{x}_2 + \ddot{x}_1) + c_2\dot{x}_2 + k_{21}x_2 + k_{23}x_2^3 = -m_2\ddot{x}_g + u_2 \end{cases} \tag{39}$$

where x_1 and x_2=interstory drifts of the first and second story, respectively; u_1 and u_2 are the control forces for the first and second floor, respectively. The structural parameters are assumed as $m_1=m_2=1{,}000$ kg, $c_1=c_2=600$ N·s/m, $k_{11}=1.2\times10^5$ N/m, $k_{13}=2\times10^7$ N/m^3, $k_{21}=6\times10^4$ N/m, and $k_{23}=5\times10^6$ N/m^3.

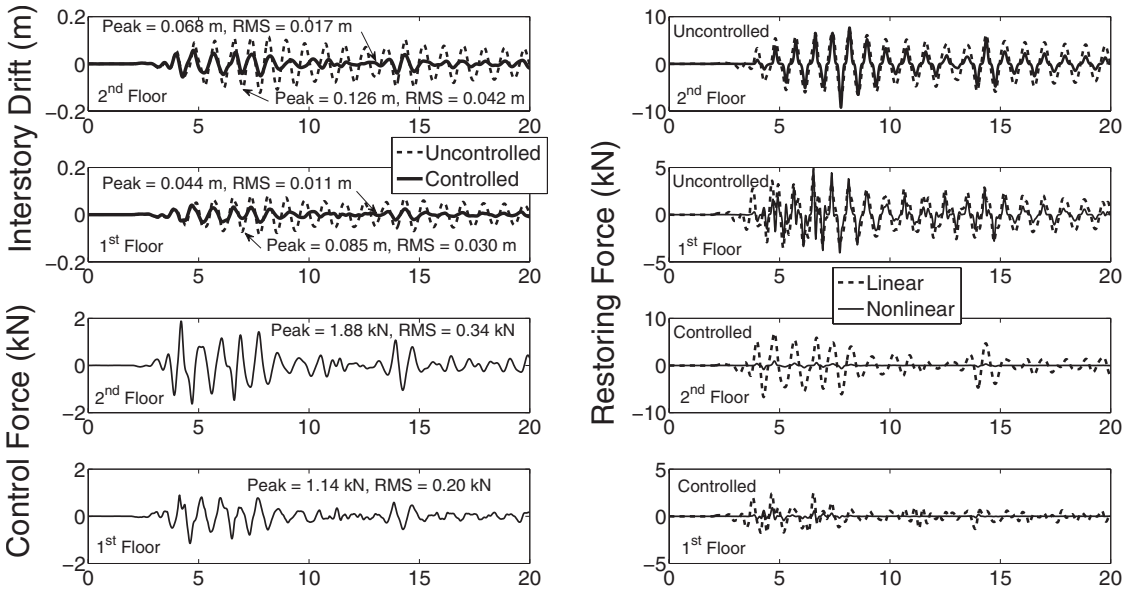

Fig. 7. Time histories of representative structural response of the two-story nonlinear elastic building subject to the full-scale 1940 El Centro earthquake

Note that the nonlinear stiffness coefficients (k_{13} and k_{23}) are selected such that under the earthquake considered, i.e., the 1940 El Centro earthquake, the nonlinear restoring forces are comparable to their linear counterparts in order to evaluate the robustness of the proposed method. The natural frequencies of the corresponding linear system are 5.93 and 14.30 rad/s with the damping ratios being 2.2 and 5.4%, respectively. The system is decomposed as

$$\begin{cases} m_1\ddot{x}_1 + c_1\dot{x}_1 + k_{11}x_1 + k_{13}x_1^3 = \tau_1 = u_1 - m_1\ddot{x}_g + c_2\dot{x}_2 + k_{21}x_2 + k_{23}x_2^3 \\ m_2\ddot{x}_2 + c_2\dot{x}_2 + k_{21}x_2 + k_{23}x_2^3 = \tau_2 = u_2 - m_2\ddot{x}_g + m_2\ddot{x}_1 \end{cases} \tag{40}$$

Control forces are assumed to be limited by 2 kN (20% story weight). The control parameters are thus selected as $\delta = 800$ N, $L = 800$ N·s/m, and $\varepsilon = 800$ N·m/s. The time histories of the interstory drifts and the control forces for the full-scale El Centro earthquake are shown in Fig. 7. The linear and nonlinear portions of the restoring forces of both floors are also shown in Fig. 7. It is seen that the interstory drifts are significantly reduced with the peak control force (1.88 kN) under the prescribed value (2 kN). The peak accelerations of both floors are also reduced significantly from 0.88 g (first floor) and 1.48 g (second floor) to 0.46 and 0.59 g, respectively. Note that with the assumed nonlinear stiffness coefficients, the nonlinear effect is quite apparent as manifested by the magnitudes of the nonlinear portion of the restoring force shown in Fig. 7. In this example, the controllers have been designed completely without the knowledge of the level of system nonlinearity and yet their effectiveness is still apparent. As a comparison, a passively controlled case is considered in which significant damping is added to every floor such that the damping coefficient is $c_1 = c_2 = 2{,}400$ N·s/m, resulting in the modal damping ratios to be 8.87 and 21.52%. The resulted peak interstory drifts are 0.049 and 0.071 m for the first and second floor, respectively. The absolute accelerations are 0.34 g (first floor) and 0.63 g (second floor).

Twenty-Story Benchmark Model

The third example considered in this study is a 20-story elastic benchmark model (Spencer et al. 1998a). This model is based on a 20-story steel frame building designed according to seismic codes for the Los Angeles, California region. There are five bays, 284 elements, and 180 joints in this benchmark frame. In the evaluation model, the number of degrees of freedom is reduced from the original number of 526 to 106. The source code is available in Spencer et al. (1998b). The first three natural frequencies of the model are 1.63, 4.71, and 8.17 rad/s, respectively. The corresponding damping ratios are 2, 5, and 10%, respectively.

The frame is decomposed into 20 subsystems, every floor level being a subsystem. Actuators are assumed to be located on every floor of the center bay. Controllers are designed in the same way for all floors. Parameter Λ is selected according to the first natural frequency of the model, i.e., $\Lambda = 5 > 1.63$ rad/s. The control force at a single floor is limited by 400 kN, which is approximately 8% of the story weight. The control parameters are then determined as $L = 100$ kN·s/m, $\delta = 100$ kN, and $\varepsilon = 100$ kN·m/s. The full-scale El Centro earthquake is used in this example to excite the structure. The numerical results are shown in Fig. 8. It is seen here that the structural responses in displacement (relative to ground) and interstory drift are noticeably reduced as compared to the uncontrolled case. Reduction rate ranges from 4 to 26%. Structural accelerations, however, are reduced at a lower level. The peak accelerations of floors one to three are slightly larger than those in the uncontrolled case. The maximum percent reduction of acceleration is 37%, occurring on the 16th floor. The maximum control force required is on the roof, with the peak and RMS values to be 142 and 51 kN, respectively. The actuators between the ground and the first floor are requested with the largest force, with the peak and RMS values of the total requested force being 2,173 and 607 kN, respectively.

The ability of this method to effectively accommodate strongly uncertain structural properties, as in the case of this benchmark finite element model, while still delivering effective control result

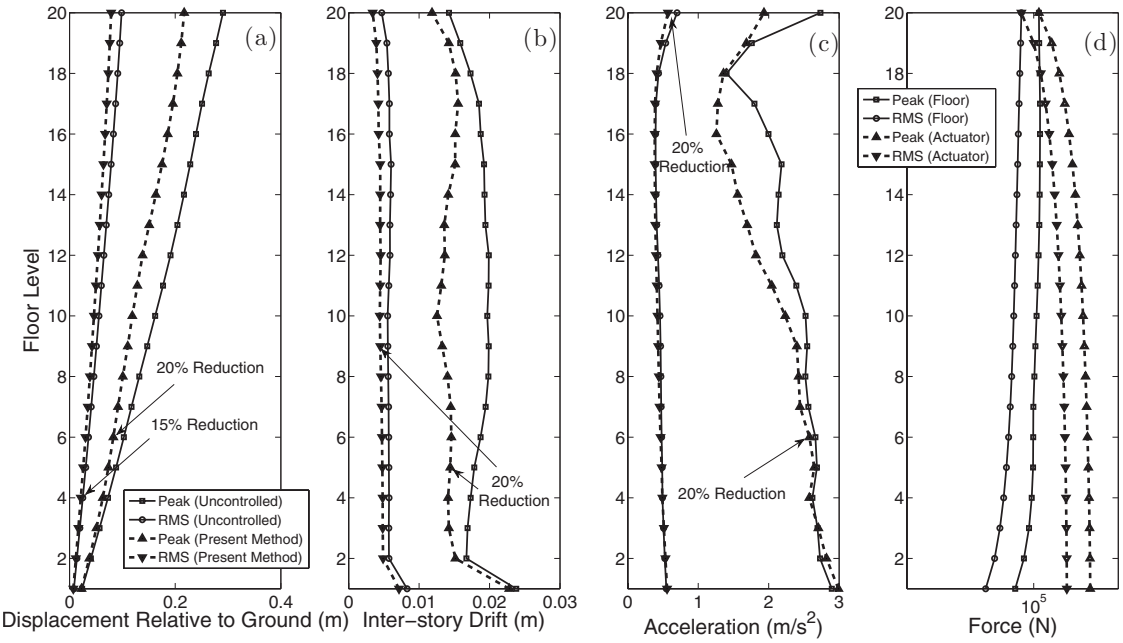

Fig. 8. Structural response and control forces of the 20-story benchmark model subject to the full-scale 1940 El Centro earthquake (actuators assumed to be placed on every floor of center bay)

is an improvement over the previous method. Using the previous method, the controller is seen to be effective for the cases where uncertainties in structural parameters are somewhat moderate or with simple patterns, e.g., uncertain lumped parameters. For this large-scale example, the previous method does not seem to find an effective control law.

It is noted that if a traditional centralized method is used to design a controller for this model, a design model with reduced order (e.g., 20 states) is usually needed as the full evaluation model (212 states) may be too large for controller design. The centralized controller designed using the reduced-order model may not perform as well as expected when the controller is designed to be very "aggressive," e.g., allowing very large control forces, because the controller becomes less robust for a more aggressive design. In the proposed approach, however, a controller performs better when it is more aggressive because the condition for convergence [see Eq. (19)] is more likely to be strictly satisfied in a more aggressive control design. When such condition is satisfied, the influence of control force on the structural behavior surpasses that of the excitation and interconnection strength, thus significant response reduction can be achieved.

Concluding Remarks

In this paper, an improved decentralized control method has been proposed for controlling multistory buildings subject to seismic excitations. Numerical simulations with results obtained from the three illustrative examples have demonstrated that this decentralized method possesses the following features:

- Prior knowledge about parameters of structural model such as material and geometrical properties is not required for control force determination;
- The proposed decentralized control law is simpler than the previous one (Ma et al. 2008) and hence more beneficial for real-time structural control application;
- Controllers designed using the proposed method utilize only the local information and hence greatly reduce the communication load of the control system; and
- Controllers can be design without the need of system identification for a structural model, whether with reduced order or not. This feature makes the proposed method more advantageous in applications of large-scale, complex system over many tradition centralized control methods.

The presented study is an initial attempt in applying the decentralized control method to achieve earthquake resistant design in civil structures. A logical next step of the study may include optimization of subsystem decomposition, control design with more accessible local feedback information (absolute acceleration instead of displacement and velocity), different ways of control force implementation, as well as diverse types of structural failure or damage.

Acknowledgments

This research is supported by NSF Grant No. CMS0511046 (Dr. S. C. Liu the program director) and the RTRF funds of University of Hawaii. Dr. Yu Tang is also gratefully acknowledged for his insightful discussion and clarification on the control theory.

References

Adhikari, R., Yamaguchi, H., and Yamazaki, T. (1998). "Modal space sliding-mode control of structures." *Earthquake Eng. Struct. Dyn.*, 27(11), 1303–1314.

Balas, G. J. (1998). "Synthesis of controllers for the active mass driver system in the presence of uncertainty." *Earthquake Eng. Struct. Dyn.*, 27(11), 1189–1202.

Brown, A. S., Ankireddi, S., and Yang, H. T. Y. (1999). "Actuator and sensor placement for multiobjective control of structures." *J. Struct. Eng.*, 125(7), 757–765.

D'Amato, F. J., and Rotea, M. A. (1998). "Limits of achievable perfor-

mance and controller design for the structural control benchmark problem." *Earthquake Eng. Struct. Dyn.*, 27(11), 1203–1224.
Dyke, S. J., Spencer, B. F., Sain, M. K., and Carlson, J. D. (1998). "An experimental study of mr dampers for seismic protection." *Smart Mater. Struct.*, 7, 693–703.
Johansen, J. D. (2008). "Active control of frame structures: A decentralized approach." Ph.D. thesis, Univ. of California, Santa Barbara, Calif.
Johnson, E. A., Voulgaris, P. G., and Bergman, L. A. (1998). "Multiobjective optimal structural control of the Notre Dame building model benchmark." *Earthquake Eng. Struct. Dyn.*, 27(11), 1165–1187.
Lu, J., and Skelton, R. R. (1998). "Covariance control using closed-loop modeling for structures." *Earthquake Eng. Struct. Dyn.*, 27(11), 1367–1383.
Lynch, J. P., and Law, K. H. (2002). "Market-based control of linear structural systems." *Earthquake Eng. Struct. Dyn.*, 31, 1855–1877.
Ma, T. W., Xu, N. S., and Tang, Y. (2008). "Decentralized robust control of building structures under seismic excitations." *Earthquake Eng. Struct. Dyn.*, 37(1), 121–140.
Ma, T. W., Yang, H. T. Y., and Chang, C. C. (2005). "Structural damage diagnosis and assessment under seismic excitations." *J. Eng. Mech.*, 131(10), 1036–1045.
Martin, C., and Soong, T. T. (1976). "Modal control of multistory structures." *J. Eng. Mech.*, 102(4), 613–623.
Mei, G., Kareem, A., and Kantor, J. (2001). "Real-time model predictive control of structures under earthquakes." *Earthquake Eng. Struct. Dyn.*, 30(7), 995–1019.
Nishitani, A., Nitta, Y., and Ikeda, Y. (2003). "Semiactive structural-control based on variable slip-force level dampers." *J. Struct. Eng.*, 129(7), 933–940.
Reinhorn, A. M., et al. (1992). "Active bracing system: A full scale implementation of active control." *Technical Rep. No. NCEER 920020*, National Center for Earthquake Engineering Research, SUNY Buffalo, N.Y.
Rohman, M., and Leipholz, H. H. (1978). "Structural control by pole assignment." *J. Eng. Mech.*, 104, 1157–1175.
Spencer, B. F., Christenson, R. E., and Dyke, S. J. (1998a). "Next generation benchmark control problem for seismically excited building." *Proc., 2nd World Conf. on Structural Control*, T. Kobori, Y. Inoue, K. Seto, H. Iemura, and A. Nichitani, eds., Wiley, New York, 1351–1360.
Spencer, B. F., Christenson, R. E. and Dyke, S. J. (1998b). "Second generation benchmark control problem for seismically excited buildings," ⟨http://sstl.cee.illinois.edu/benchmarks/bench2def/⟩ (Feb. 2010).
Spencer, B. F., Suhardjo, J., and Sain, M. K. (1994). "Frequency domain optimal control strategies for aseismic protection." *J. Eng. Mech.*, 120(1), 135–158.
Tang, Y., Tomizuka, M., Guerrero, G., and Montemayor, G. (2000). "Decentralized robust control of mechanical systems." *IEEE Trans. Autom. Control*, 45(4), 771–776.
Whorton, M. S., Calise, A. J., and Hsu, C. C. (1998). "A study of fixed-order mixed norm designs for a benchmark problem in structural control." *Earthquake Eng. Struct. Dyn.*, 27(11), 1315–1330.
Wu, J. C., Yang, J. N., and Agrawal, A. K. (1998). "Applications of sliding mode control to benchmark problems." *Earthquake Eng. Struct. Dyn.*, 27(11), 1247–1265.
Xu, B., Wu, Z. X., and Yokoyama, K. (2003). "Neural networks for decentralized control of cable-stayed bridge." *J. Bridge Eng.*, 8(4), 229–236.
Xu, N. S., and Yang, Z. H. (1999). "Predictive structural control based on dominant internal model approach." *Automatica*, 35(1), 59–67.
Yang, J. N. (1975). "Application of optimal control theory to civil engineering structures." *J. Eng. Mech.*, 101, 819–838.
Yang, J. N. (1982). "Control of tall buildings under earthquake excitation." *J. Engrg. Mech. Div.*, 108(5), 883–849.
Yang, J. N., and Lin, S. (2005). "Identification of parametric variations of structures based on least squares estimation and adaptive tracking." *J. Eng. Mech.*, 131(3), 290–298.
Yao, J. T. P. (1972). "Concept of structural control." *J. Struct. Div.*, 98(7), 1567–1574.
Young, P. M., and Bienkiewicz, B. (1998). "Robust controller design for the active mass driver benchmark problem." *Earthquake Eng. Struct. Dyn.*, 27(11), 1149–1164.